Study of the Structure and Mechanism of Formation through Self-Assembly of Mesostructured Vanadium Oxide

Victor Luca*,† and James M. Hook‡

School of Chemistry and NMR Facility, University of New South Wales, Sydney 2052, Australia

Received December 17, 1996. Revised Manuscript Received June 16, 1997⊗

The structure and mechanism of formation of a novel hexagonal mesostructured vanadium oxide−surfactant composite (HMVO), synthesized by acid-catalyzed hydrolysis of ethanolic cetyltrimethylammonium vanadate (CTAV) solution, has been studied by a variety of spectroscopic techniques. The poorly crystalline CTAV precursor used in the synthesis has been characterized and is shown to consist of pyrovanadate-like anions in which one oxygen atom is shared between vanadate tetrahedra. The HMVO formed from this precursor appears to feature a distorted octahedral vanadium coordination similar to that found in extended structures such as the two-dimensional vanadium pentoxide gel network. Information on the solution speciation during the synthesis is monitored by ^{51}V NMR spectroscopy. Prior to acid addition, the ethanolic solution of CTAV shows a single narrow resonance at −556.7 ppm, assigned to a tetrahedral diester anion $[VO_2(OEt)_2]^-$, undergoing fast reorientational averaging of the quadrupole interaction in solution. This behavior indicates that mesophases do not exist in solution prior to the initiation of acid-catalyzed polymerization. Progressive addition of aqueous acid results in a monotonic decrease in the diester concentration with concomitant formation of minor quantities of higher vanadate oligomers and an increasing proportion of mesophase not directly detectable by solution ^{51}V NMR. The water in the aqueous acid plays an important role as an initiator in the hydrolysis of the diester, producing the higher oligomers, as well as a postulated transitory intermediate, which condenses rapidly through the action of the stronger acid, HCl, and directed by the surfactant to give the mesostructured material. The presence of the surfactant is seen to be crucial for inhibiting the formation of anionic decavanadate clusters, and VO_2^+ species, which are normally associated with the acidification of aqueous vanadate solutions. These observations are consistent with a formation mechanism in which the vanadium mesophase is generated by cooperative formation of micellar entities and higher vanadate oligomers.

Introduction

In organic chemistry simple molecular building blocks can be put together with predictability and exquisite control, making it possible to realize complex molecular entities using relatively simple reaction schemes. This is not so in the synthesis of aluminosilicates and other inorganic molecular sieve structures which usually involves a series of complex polymerization/condensation reactions which are poorly understood and notoriously difficult to control. Using mainly trial and error methods, the past decade has seen the synthesis of many new molecular sieve structures using individual organic molecules as structure directing or templating agents. Thus the inorganic framework assembles around the organic entity which in most cases plays a space-filling role rather than acting as a genuine template. By templating it is meant that the structure of the organic defines the structure of the inorganic framework and therefore the molecular sieve. Of the molecular sieves synthesized so far, there are only a few known examples where the organic acts in this capacity.[1]

Although nature routinely uses self-assembled organic scaffolds to build complex ceramics of nanometer dimensions, materials scientists have only recently exploited surfactant self-assembly to perform templated inorganic syntheses. Notably, such chemistry was recently demonstrated by workers at Mobil Corp. in the syntheses of aluminosilicates with nanometer size pores[2−4] where the ability of surfactant micelles to assemble into large hexagonal aggregates was utilized. The usual starting material for these syntheses is a solution containing polymeric Al and Si species of ranging nuclearity. More recently, however, it was shown that MCM-41 materials could also been assembled in a "cleaner" fashion using single octomeric silicate ($Si_8O_{20}^{8-}$) and aluminate anions, which in solu-

* To whom correspondence should be addressed: School of Chemistry, University of New South Wales, Sydney 2052, Australia. Tel: 61-2-9385 4678. Fax: 61-2-9385 6141. E-mail: v.luca@unsw.edu.au or s9500124@pop3.unsw.edu.au.

† School of Chemistry.

‡ NMR Facility.

⊗ Abstract published in *Advance ACS Abstracts,* October 15, 1997.

(1) Davis, M. E.; Lobo, R. F. *Chem. Rev.* **1992**, *4*, 756.

(2) (a) Kresge, C. T.; Leonowicz, M. E.; Roth, W. J.; Vartuli, J. C., U.S. Patent 5 098 684, 1992. (b) Beck, J. S.; Chu, C. T.-W.; Johnson, I. D.; Kresge, C. T.; Leonowicz, M. E.; Roth, W. J.; Vartuli, J. C. U.S. Patent, 5 108 725, 1992.

(3) Kresge, C. T.; Leonowicz, M. E.; Roth, W. J., Vartuli, J. C. U.S. Patent 5 102 643, 1992.

(4) Beck, J. S.; Vartuli, J. C.; Roth, W. J.; Leonowicz, M. E.; Kresge, C. T.; Schmitt, K. D.; Chu, C. T.-W.; Olson, D. H.; Sheppard, E. W.; McCullen, S. B.; Higgins, J. B.; Schlenker, J. L. *J. Am. Chem. Soc.* **1992**, *114*, 10834.

S0897-4756(96)00641-2 CCC: $14.00

tion exchange for the initial surfactant counterions (usually Cl^- or Br^-).[5,6]

There has been much interest recently in the template-directed synthesis of open framework vanadium oxides and phosphates[7] as well as the synthesis of vanadium-substituted zeolite and molecular sieve structures. Such interest is fueled by the exceptional performance of vanadium-based oxide catalysts in a number of commercially important reactions. It was therefore natural to attempt to incorporate vanadium into the structure of the aforementioned mesoporous silicates, and indeed a number of studies have reported results of such endeavors.[8−12]

Rather than incorporating transition metals into siliceous M41S materials, others have attempted to synthesize pure mesoporous transition metal oxide and phosphate analogues by utilizing surfactant self-assembly.[13−15] These materials were thermally unstable, and more recently mesostructured tantalum[16] and niobium oxides[17,18] have been synthesized from which the surfactant template can be removed by treatment with hot HCl/ethanol solutions to yield mesoporous materials. These materials represent some of the few all transition metal analogues of M41S materials for which the template can be relatively easily removed.

An interesting situation has been reported by Stein et al.[13] who showed that, in attempting to synthesize mesostructured tungsten oxide phases using heteropolytungstate salts of cetyltrimethylammonium (CTA), materials were produced that gave lattice images reminiscent of M41S materials but for which FTIR measurements showed unequivocally the presence of only the intact and unconnected heteropolytungstate anions. This raises the possibility of a more general chemistry between anionic polyoxometalate species and surfactant micelles in which M41S-like materials are produced.

Our approach to synthesize mesoporous vanadium oxides utilized monomeric precursors, with the aim of controlling the condensation of these monomers by performing reactions in nonaqueous solvents and was recently reported in this journal.[19] This was the first synthesis of mesophase material commencing with an ethanolic solution containing only the cationic surfactant and essentially isolated monomeric vanadate counterions. The starting point for the synthesis was first isolation of the cetyltrimethylammonium vanadate precursor which was then dissolved in ethanol, affording a solution comprised mainly of vanadate monomers as shown by NMR. These monomers could then be polymerized and condensed through the controlled addition of HCl; the resulting phase was mesostructured and showed many features in common with M41S aluminosilicate materials including a hexagonal structure. The surfactant template in this material could not be removed by thermal treatment in air without structural decomposition, and there have been no other reports of the synthesis of thermally stable mesoporous vanadium oxides using the surfactant route. Because of its poor thermal stability we termed this material mesostructured vanadium oxide (MVO) as was done by Stein et al.[13] in reference to tungsten mesophase materials. We now refer to it as hexagonal mesostructured vanadium oxide (HMVO) to distinguish it from layered mesophases.

Table 1. Chemical Compositions of CTA−Vanadates and HMVO

compd	composition
CTAV1	$C_{19.0}H_{44.6}N_{0.97}V_{0.63}$
CTAV3	$C_{19.0}H_{45.6}N_{1.0}V_{0.792}$
CTAV5	$C_{19.0}H_{42.2}N_{0.7}V_{1.56}$
HMVO	$C_{19.0}H_{43.1}N_{0.9}V_{2.28}$

Very recently Janauer et al.[20] attempted to synthesize mesostructured vanadium oxide phases using dodecyltrimethylammonium bromide but produced instead a new crystalline layered vanadium oxide/surfactant composite which they characterized in detail. Although the layered vanadium oxide material synthesized by these workers has an XRD pattern that is quite different from that of HMVO reported by us, they have highlighted the need for more precise characterization of transition metal oxide/surfactant composites. In the present study we complete the characterization of HMVO that we reported previously and attempt to shed light on the mechanism by which this mesostructured oxide forms.

Experimental Section

In a typical synthesis of HMVO, the vanadate salt of the cetyltrimethylammonium cation was first isolated by adding excess CTA−chloride (Fluka) to a 0.115 M solution of ammonium vanadate (Aldrich). The pH of this solution prior to addition of CTA−chloride was 6.5. The resulting white precipitate was filtered, washed thoroughly with distilled water, and dried at 40 °C. The product (CTAV3) has the composition shown in Table 1, indicating that there is roughly one vanadium per surfactant anion; chloride was absent. Attempts to date to obtain crystals of CTA−vanadate suitable for single-crystal X-ray analysis have been unsuccessful.

The solid CTA−vanadate (3.21 g) was dissolved in ethanol (240 mL) to give a solution that was 35 mM in vanadium concentration and an initial pH between 8.0 and 9.0. This solution was then titrated at ambient temperature with 0.20 M HCl past the end point (pH = 4.5) to a pH of 2.2. Continued addition of acid past this point yielded X-ray amorphous products. After completion of the titration the red-brown precipitate that formed was filtered, washed thoroughly, first with ethanol and then distilled water, and finally air-dried. In a previous study it was shown that this compound has a structure similar to that of M41S materials.[19] In order to facilitate comparison of the results of different preparations

(5) Fyfe, C. A.; Fu, G. *J. Am. Chem. Soc.* **1995**, *117*, 9709.
(6) Fu, G.; Fyfe, C. A.; Schwieger, W.; Kokotailo, G. T. *Angew. Chem., Int. Ed. Engl.* **1995**, *34*, 1499.
(7) Bu, X.; Feng, P.; Stucky, G. D. *J. Chem. Soc., Chem. Commun.* **1995**, 1337.
(8) Luan, Z. H.; Xu, J.; He, X. Y.; Klinowski, J.; Kevan, L. *J. Phys. Chem.* **1996**, *100*, 10505.
(9) Reddy, K. M.; Moudrakovski, I.; Sayari, A. *J. Chem. Soc., Chem. Commun.* **1994**, 1059.
(10) Reddy, J. S.; Sayari, A. *J. Chem. Soc., Chem. Commun.* **1995**, 2231.
(11) Reddy, K. M.; Moudrakovski, I.; Sayari, A. *J. Chem. Soc., Chem. Commun.* **1994**, 1059.
(12) Reddy, K. M.; Moudrakovski, I.; Sayari, A. *J. Chem. Soc., Chem. Commun.* **1994**, 1491.
(13) Stein, A.; Fendorf, M.; Jarvie, T. P.; Mueller, K. T.; Benesi, A. J.; Mallouk, T. E. *Chem. Mater.* **1995**, *7*, 304.
(14) Cielsa, U.; Demuth, D.; Leon, R.; Petroff, P.; Stucky, G. D.; Unger, K.; Scuth, F. *J. Chem. Soc., Chem. Commun.*, **1994**, 1387.
(15) Knowles, J. A.; Hudson, M. J. *J. Chem. Soc., Chem. Commun.* **1995**, 2083.
(16) Antonelli, D. M.; Ying, J. Y. *Chem. Mater.* **1996**, *8*, 874.
(17) Antonelli, D. M. ; Ying, J. Y. *Angew. Chem., Int. Ed. Engl.* **1996**, *35*, 426.
(18) Antonelli, D. M.; Nakahira, A.; Ying, J. Y. *Inorg. Chem.* **1996**, *35*, 3126.
(19) Luca, V.; MacLachlan, D. J.; Hook, J. M.; Withers, R. *Chem. Mater.* **1995**, *7*, 2220.
(20) Janauer, G. G.; Dobley, A.; Guo, J.; Zavalij, P.; Whittingham, M. S. *Chem. Mater.* **1996**, *8*, 2096.

using different initial volumes of ethanolic CTA−vanadate solution, the amount of acid added will be given in terms of the mole fraction of water R defined as R = moles of H_2O/(moles of H_2O + moles of ethanol).

Room-temperature wide-line solid-state ^{51}V NMR studies were carried out at 78.9 MHz on a Bruker MSL 300 spectrometer. According to previous recommendations, pulse lengths of 1 μs or less are most suitable for relative signal quantification.[21] Thus a 0.6 μs (15°) pulse length and 1 s recycle delay was used to record the static spectra. Magic angle spinning (MAS) spectra were recorded at 12 and 10 kHz spinning speed and the isotropic shifts (uncorrected for second-order quadrupolar shift) obtained by comparison of these spectra. Similar pulse lengths and recycle delays were used as for the acquiring the MAS spectra.

Solution ^{51}V NMR studies were carried out on a Bruker ACP 300 spectrometer using a 10 mm broad band probe tuned to 78.9 MHz . All chemical shifts are reported with respect to $VOCl_3$ (0 ppm).

Raman spectra were recorded on a Renishaw Raman microscope using an argon ion laser (λ = 514.5 nm). Spectra were recorded at the lowest possible laser power level consistent with acceptable signal-to-noise ratio in order to avoid effecting changes to the nature of the surface species due to sample heating by the laser beam.

X-ray absorption spectra were recorded at the Photon Factory, Tsukuba, Japan, on beam line 20B. A Si(111) monochromator crystal was used, and this was detuned about 40% for harmonic rejection. In the X-ray absorption near-edge structure (XANES) region between 4940 and 5020 eV, energy was scanned in 0.10 eV steps, while in the extended X-ray absorption fine structure (EXAFS) region, energy was scanned in 2.2 eV steps between 5020 and 5460 and 4.5 eV steps between 5460 and 6000 eV. The energy scale was calibrated with respect to the maximum of the first preedge peak of a vanadium metal foil which was assigned an energy of 5464 eV. Energy resolution was such that the peak-to-peak first derivative line width of the first preedge feature in the vanadium metal foil spectrum was equal to 1.35 eV. Analysis of the EXAFS was performed using the program XFIT.[22] The edge step of the XANES spectra were normalized to one by fitting a zero-order polynomial to a selected energy range in the postedge region.

FTIR spectra were acquired on a Perkin-Elmer PE1800 spectrometer with samples pressed in KBr disks.

XRD patterns were recorded on a Siemens D500 diffractometer using a Cu Kα radiation and a graphite monochromator. Samples were examined as randomly oriented powders or in the case of surfactant solutions as films. The latter were deposited by allowing several drops of the surfactant solution to spread on the surface of clean borosilicate microscope slides held in the horizontal position. The continuous even layer of solution that resulted from this procedure was allowed to dry in ambient air to give continuous transparent films.

Measurements of pH were made with a standard pH meter and a combination electrode that had been standardized with aqueous buffer solutions. It has been shown that hydrogen ion concentrations in ethanol−water mixtures can be measured accurately with a correction factor of −0.032 to 0.221 log units in solvents with 86% or less ethanol.[23] A somewhat larger uncertainty can be expected for higher ethanol concentrations, but this should be tolerable given the accuracy required in the present experiments.

Results and Discussion

1. Synthesis and Characterization of CTA−Vanadate Salts. CTA−vanadate has so far resisted crystallization, and the stoichiometry published previously[19] shows that there is close to one vanadium for each surfactant anion. This however gives little indication of the nuclearity of the vanadate counterion. Therefore, as a starting point we examined in detail the chemistry of the precursor compounds and the initial vanadate solutions from which they derived to provide important information on the structure of the precursor compounds, their relationship to the solutions from which they derived, and finally for comparison with the structures of the final products.

^{51}V Solution NMR. The predominance diagram for vanadates in aqueous solution is shown in Figure 1a. V-51 NMR spectra corresponding to solutions with pH and vanadium concentration in each of the six regions indicated in Figure 1a are shown in Figure 1b. The definitive assignments of the NMR resonances are from previous work.[24,25] CTA−vanadate used for the synthesis of the mesostructured vanadium oxide phase was obtained from a solution with concentration and pH plotting in region 3. In region 1, isolated monomeric tetrahedral vanadate ions are expected and these give a single NMR peak of very narrow line width (fwhm = 52 Hz) . The chemical shift of the monomeric vanadate depends on the state of protonation, i.e., the value of x in $H_xVO_4^{3-x}$ varies in the range 0 to 2. Both the narrow line width and chemical shift characterize this symmetrical tetrahedral molecule. Three principal species are found in region 2 and they are the monomer (V1), the dimer (V2), and the tetramer (V4). The region 3 solution is cleaner in the sense that only the V4 and V5 species are found in solution while in region 4, the decavanadate ion predominates, though an assortment of smaller oligomers including mainly V4 can also be observed. The three resonances observed in the spectrum of the region 5 solution can be assigned to the triprotonated form of the decavanadate ion $H_3V_{10}O_{28}^{3-}$ (V10). It cannot be excluded however that less protonated forms of the cluster are also present but that these evade detection because of rapid exchange with solvent protons.[26]

Solid CTA−vanadates were isolated by adding an excess of CTA−chloride to solutions from regions 1, 3, and 5 and filtering, washing with copious water, and air-drying. These will be denoted CTAV1, CTAV3, and CTAV5. The CTAV1 powder was off-white, the CTAV3 was very pale yellow, CTAV5 was bright yellow-orange, and their chemical compositions are listed in Table 1. These solids were further characterized by a variety of techniques described below. Although CTAV1 and CTAV3 were soluble in methanol, ethanol, and higher alcohols, CTAV5 could not be dissolved in any common organic solvents.

X-ray Diffraction. Powder XRD patterns of CTAV1, CTAV3, and CTAV5 are shown in Figure 2. Both CTAV1 and CTAV3 samples contain a major phase with most intense reflection at about 26 Å while three low angle reflections are observed in the XRD pattern of the CTAV5 sample having d-spacings of 25.4, 24.6, and 23.0 Å. Higher order basal plane harmonics can be observed for CTAV5 at 12.6, 12.2, and 11.4 Å corresponding to the n + 1 order reflections of these layered phases. Higher harmonics out to the fourth order can also be

(21) Eckert, H.; Deo, G.; Wachs, I. E.; Hirt, A. M. *Colloids Surf.* **1990**, *45*, 347.
(22) Ellis, P. A.; Freeman, H. C. *J. Synchrotron Rad.* **1995**, *2*, 190.
(23) Gresser, M. J.; Tracey, A. S. *J. Am. Chem. Soc.* **1985**, *107*, 4215.
(24) Howarth, O. W. *Prog. NMR Spectrosc.* **1990**, *22*, 453.
(25) Heath, E.; Howarth, O. W. *J. Chem Soc., Dalton Trans.* **1981**, 1105.
(26) Pozarnsky, G. A.; McCormack, A. V. *Chem. Mater.* **1994**, *6*, 380.

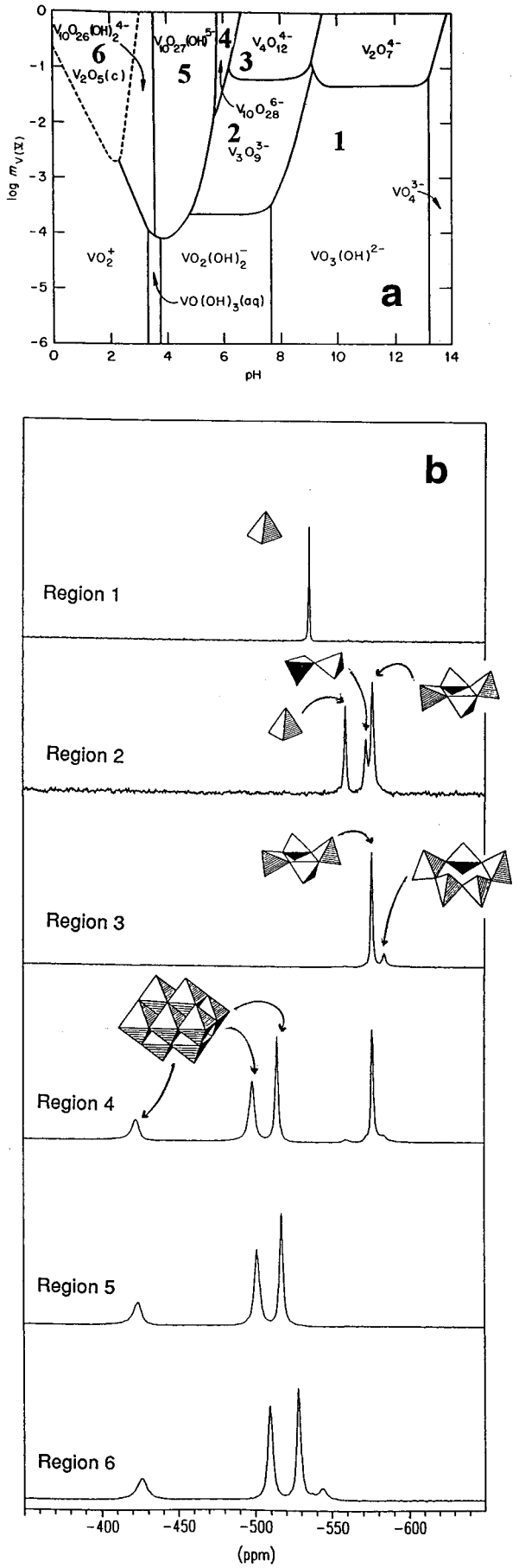

Figure 1. (a) Predominance diagram for V(V)−OH− species at 25 °C (adapted from Baes and Mesmer, 1976). (b) Solution ^{51}V NMR spectra of vanadate solutions selected from the concentration−pH regions marked (a).

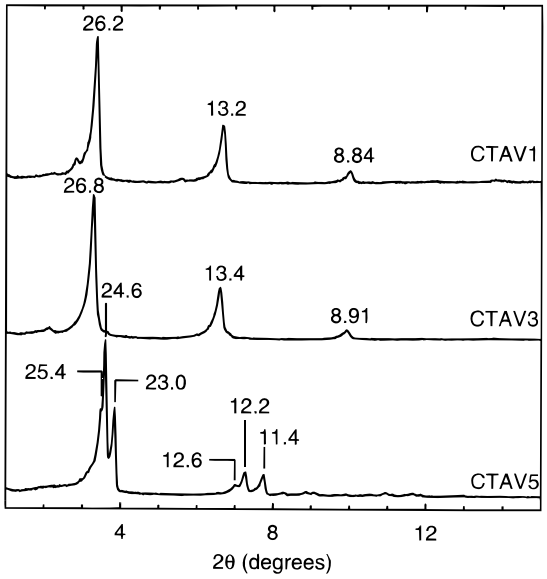

Figure 2. XRD powder patterns of CTAV1, CTAV3, and CTAV5 samples isolated by adding CTA−chloride to solutions from region 1, 3, and 5 of Figure 1a, respectively.

observed by closer inspection. These results indicate that while essentially single phases are formed from solutions in region 1 and 3, the product from region 5 contains three layered phases. One possible explanation for this could be that the $H_xV_{10}O_{28}^{6-x}$ anions in CTAV5 are protonated to different degrees giving a different charge on the cluster. This requires different numbers of CTA^+ counterions per vanadate cluster ion which then influences chain packing and therefore interlayer space.

The XRD pattern of a CTAV3 film (not shown) was similar to that obtained for the powder shown in Figure 2 with the most intense reflection also occurring at 26.5 Å. This can be compared with the XRD pattern of a CTA−chloride film (not shown) which also indicates a layered structure from a series of basal plane harmonics in its powder pattern, but the lowest order reflection is observed at 32.5 Å. This is probably not the 001 reflection and more likely corresponds to the 002 reflection by analogy with the known crystal structure of CTA−bromide. If this is so, then the 001 reflection would occur at 65 Å which is beyond the range that is accessible by our instrument. The primary reflection observed in the XRD patterns of the CTAV samples is therefore probably also the second-order reflection.

^{51}V Static and MAS Solid-State NMR. Vanadate coordination can be deduced from a combination of the isotropic chemical shielding or shift value, δ_{iso}, obtained from the MAS NMR spectrum and the anisotropy (defined as $\Delta\delta = \delta_{33} - \delta_{11}$ in this work or $\delta_{33} - \delta_{iso}$ by some) determined from static spectra.[27−29] The magnitude of the anisotropy can give an indication of the connectivity, Q^n, of the vanadium polyhedra, where n represents the number of shared oxygen atoms per tetrahedron or octahedron. Thus for a regular tetrahedron of type Q^0, where the V−O bond lengths are equal, the shift tensor components δ_{11}, δ_{22}, and δ_{33}

(27) Eckert, H.; Wachs, I. E. *J. Phys. Chem.*, **1989**, *93*, 6796.
(28) Lapina, O. B.; Mastikhin, V. M.; Shubin, A. A.; Krasilnikov, V. N.; Zamaraev, K. I. *Prog. NMR Spectrosc.* **1992**, *24*, 457.
(29) Smits, R. H. H.; Seshan, K.; Ross, J. R. H.; Kentgens, A. P. M. *J. Phys. Chem.* **1995**, *99*, 9169.

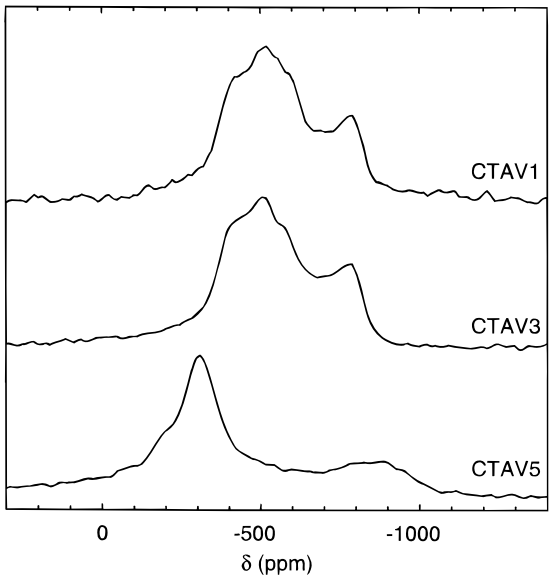

Figure 3. ^{51}V solid-state static NMR spectra of CTAV1, CTAV3, and CTAV5 isolated from region 1, 3, and 5 of Figure 1a.

are equal and the anisotropy is less than 100 ppm. For slightly distorted Q^1 type tetrahedra where one oxygen atom is shared, anisotropies between 100 and 300 ppm are observed and the shift tensor is asymmetric, $\delta_{11} \neq \delta_{22} \neq \delta_{33}$. For distorted tetrahedra of type Q,[2] anisotropies of between 400 and 600 ppm are found while the tensor remains asymmetric. Finally, for octahedral vanadium, very large anisotropies of the order of 600 to 1200 ppm obtain and the chemical shift tensor is axial, $\delta_{11} = \delta_{22} \neq \delta_{33}$.

Static ^{51}V spectra for the three CTA salts are shown in Figure 3. CTAV1 and CTAV3 have identical static NMR spectra with an asymmetric chemical shift tensor having principal components of −412, −503, and −776 ppm. Note that these values have been estimated from the spectra without simulation and so the uncertainty in the values could be as high as ±20 ppm. As discussed above, such a shift tensor is characteristic of 4-fold coordination, with a connectivity of Q^1 as judged from the anisotropy of 362 ppm. The static spectrum of CTAV5, on the other hand, shows an axial shift tensor with the main peak centered at about −300 ppm and a minor feature at about −872 ppm. Such a tensor is indicative of distorted octahedral coordination for vanadium, similar to that found for V_2O_5.[27]

MAS NMR spectra were recorded with a spinning speed of 12 kHz for the three CTAV compounds but are not shown. The spectra for CTAV1 and CTAV3 are identical with both vanadates having a single isotropic shift (uncorrected for possible quadrupolar shift) at −579 ppm and weak sideband structure. The MAS NMR spectrum of CTAV5 on the other hand is dramatically different from that of the other two CTA−vanadates. It contains four isotropic chemical shifts at −441, −489, −505, and −538 ppm, but this time with a slightly more pronounced sideband structure. These shifts are reminiscent of the solution spectrum of $V_{10}O_{28}^{6-}$ which shows resonances at −425, −498, and −515 ppm corresponding to the three structurally distinct vanadium sites in the V10 cluster. We conclude that the V10 cluster has been precipitated intact but for the present

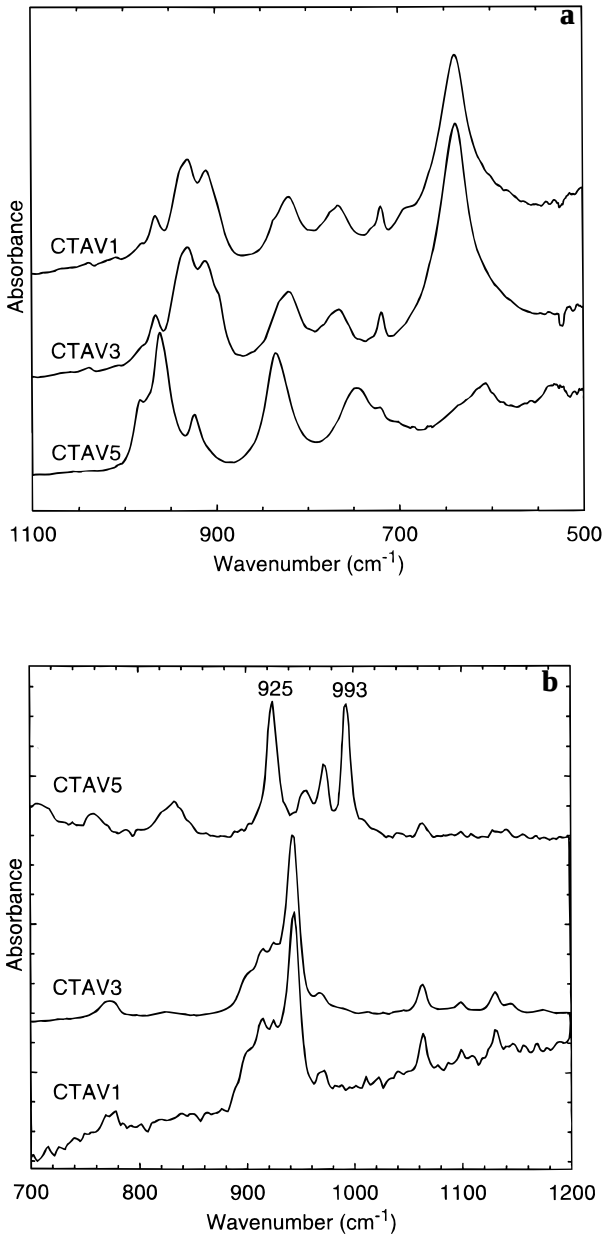

Figure 4. (a) FTIR spectra of CTAV1, CTAV3, and CTAV5. (b) Raman spectra of CTAV1, CTAV3, and CTAV5.

we cannot define the number of surfactant molecules associated with each V10 unit.

FTIR/Raman. FTIR spectra of CTA−vanadates in the range 500−1200 cm^{-1} are shown in Figure 4a. Vibrations of vanadate polyhedra occur around 930 cm^{-1}, and in this region the spectra of CTAV1 and CTAV3 contain a series of overlapping vibrations around 930 cm^{-1} that are qualitatively similar to those of the $V_2O_7^{4-}$ polyanion found in magnesium pyrovanadate.[30] In this polyanion the V coordination is tetrahedral and there is one V−O−V bridge. Weak bands between 700 and 850 cm^{-1} can be ascribed to VO_3 stretching vibrations as they are absent in FTIR spectra of CTA−chloride and CTA−bromide. In parallel with the NMR results, CTAV1 and CTAV3 have FTIR spectra that are identical. In contrast, the CTAV5 sample has an FTIR spectrum with bands at 983, 960, and 923 cm^{-1} that

(30) Busca, G.; Ricchardi, G.; Siew Hew Sam, D.; Volta, J.-C. *J. Chem. Soc., Faraday Trans.* **1994**, *90*, 1161.

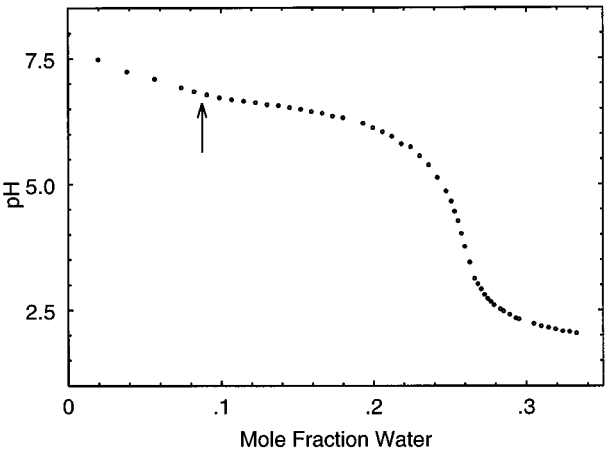

Figure 5. Curve for the titration of 35 mM ethanolic CTA−vanadate solution against 0.020 M HCl solution.

match closely the main bands of the decavanadate ion at 985, 960, and 930 cm^{-1}.[31] It is clear therefore from these data that CTAV5 corresponds to the intact and isolated decavanadate ion $H_xV_6O_{28}^{6-x}$ (V_{10}) salt of the cetyltrimethylammonium cation. Raman spectra of the three compounds (Figure 4b) also indicate that CTAV1 and CTAV3 have a similar structure on the basis of their vibrational spectrum whereas the Raman spectrum of the CTAV5 salt is clearly distinctive.

It would appear that in the synthesis of CTAV, regardless of whether the initial aqueous vanadate solution contains predominantly monomers (region 1) or predominantly tetramers (region 3), addition of CTA−chloride precipitates vanadate as a dimer, the formula of which is wholly consistent with $CTA_2V_2O_7$ inferred from the spectroscopic and analytical data. Thus the addition of CTA^+ changes the solution equilibrium dramatically, selecting exclusively the V2 species. On the other hand, when CTA−chloride is added to a solution containing predominantly the V10 anion, the intact and uncondensed cluster is incorporated into one or a series of layered mesophases.

2. Characterization of Hexagonal Mesostructured Vanadium Oxide (HMVO). A typical curve for the titration of CTA−vanadate ethanolic solution with 0.20 M HCl is shown in Figure 5. The equivalence point of this titration occurs around pH = 4.0 and precipitate is not observed until $R \sim 0.1$ (vertical arrow in Figure 5). To characterize the solid phases forming during the titration very small aliquots of suspension were removed at various intervals.

X-ray Diffraction. XRD patterns of films deposited from aliquots extracted during the titration are shown in Figure 6. Near the start of the titration the XRD pattern contains essentially a single reflection with d = 31.2 Å which is somewhere between the principle reflections observed for the pure CTA−chloride and CTA−vanadate films. As the titration progresses the relative intensity around 2.5 2θ increases with a number of poorly resolved reflections being observed. It is noteworthy that there is no change in the d-spacing of the sharp intense reflection with titration.

Washing any of the samples with ethanol prior to film deposition greatly reduces the intensity of the 31.2 Å reflection. When the unwashed films were left standing for extended periods of time, the XRD pattern changed markedly as shown in Figure 7. For the film deposited from a solution after the addition of only 0.5 mL of HCl with pH = 8.5 (Figure 7a) a single phase is observed soon after air-drying with d-spacing of 31.1 Å. After the film stands in air for several months, an additional phase with d = 52.5 Å is observed (Figure 7b). The film formed from a solution with pH = 7.11 (Figure 7c) again possesses the reflection at 31.0 Å but now an additional reflection can be observed at 38 Å. Extended air-drying of this sample generated a very complex diffraction pattern in the angle region below about 4 degrees 2θ with numerous mesophases having spacings ranging from 23 to 53 Å (Figure 7d). The XRD patterns generally became less complex as more acid was added with the phase at 38 Å eventually dominat-

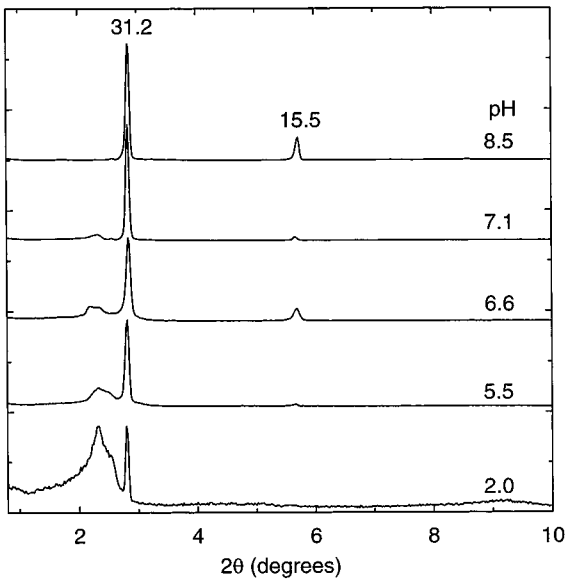

Figure 6. XRD powder patterns of CTA−vanadate films obtained from suspensions isolated at various stages of the titration of ethanolic CTA−vanadate solution with 0.020 M HCl.

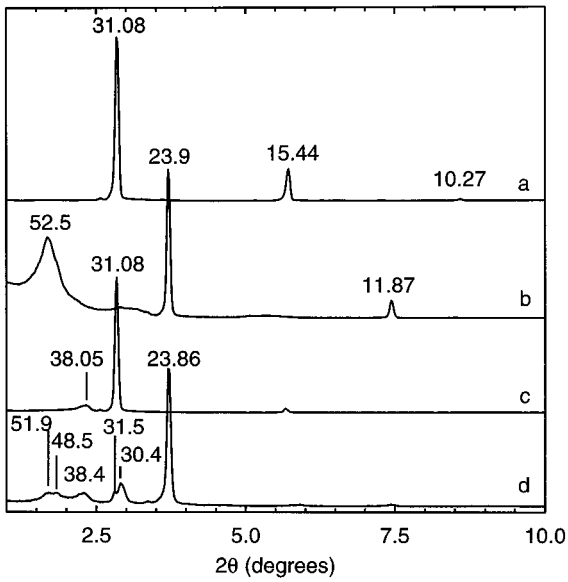

Figure 7. XRD patterns of (a) CTA−vanadate film isolated from solution with pH = 8.47, (b) sample from (a) aged for several months, (c) CTA−vanadate film isolated from solution with pH = 7.11, and (d) sample from (c) aged several months.

(31) Day, V. W.; Klemperer, W. G.; Maltbie, D. J. *J. Am. Chem. Soc.* **1987**, *109*, 2991.

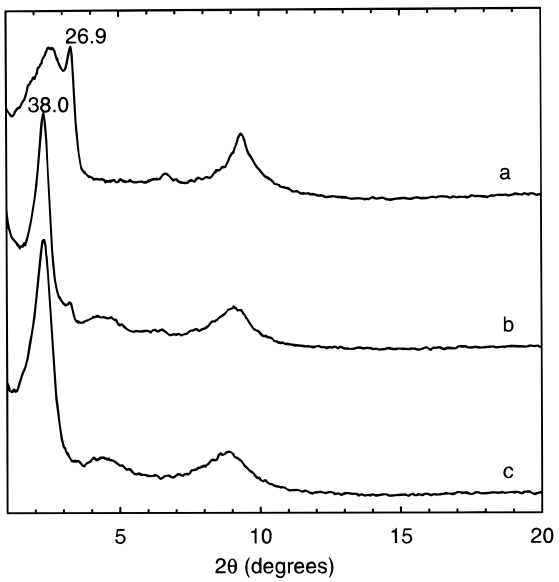

Figure 8. XRD patterns of powders isolated by centrifugation and washing with ethanol of suspensions produced during the titration of CTA−vanadate with 0.020 M HCl. Suspension pH values are (a) 6.87, (b) 5.80, and (c) 4.73.

ing the low-angle region below 4 degrees 2θ. The rich variety of phases identified in these XRD patterns suggests association of the surfactant with vanadate oligomers of various sizes and/or the variable water content of a limited number of layered mesophases.

Figure 8 shows XRD patterns of precipitates collected by filtration at various stages of the titration and subsequently washed thoroughly with ethanol and air-dried. Apart from the reflection assigned to HMVO (d = 38 Å), all other low-angle reflections are associated with higher order basal plane harmonics giving a clear indication that they are due to layered vanadate mesophases. For the precipitate collected at a pH of 6.9 (Figure 8a), washing did not eliminate all of the 26.9 Å phase, which was observed in addition to a very broad reflection at around 34.2 Å. Titration to pH = 5.8 yielded a washed precipitate that gave a principal reflection at 38.4 Å as well as additional broad reflections at 20.1 and 9.7 Å (Figure 8b). These three reflections were previously identified as originating from a hexagonal mesostructured vanadium oxide phase.[19] In this pattern there is only a small amount of the 26.9 Å phase which completely disappears on reaching pH = 4.7, leaving only the pattern of the mesostructured phase (Figure 8c). Continued titration to pH = 2.5 yields essentially the same XRD pattern, although the chemical yield is reduced.

^{51}V Solid State NMR. Figure 9a shows static spectra of HMVO and V_2O_5 gel, both of which reflect an axial chemical shift tensor with $\delta_{11} = \delta_{22}$ of about −300 ppm and variable δ_{33} for the samples investigated. This type of tensor is characteristic of the distorted octahedral coordination in which vanadium is found in these compounds. The variation in δ_{33} indicates that the degree of axial distortion of the V polyhedron differs slightly between the two compounds. The anisotropy displayed in the spectrum of HMVO is about 100 ppm less than V_2O_5 gel indicating that the vanadium coordination in the HMVO is slightly less distorted. Also, the spectrum of the gel is somewhat broader than that of HMVO.

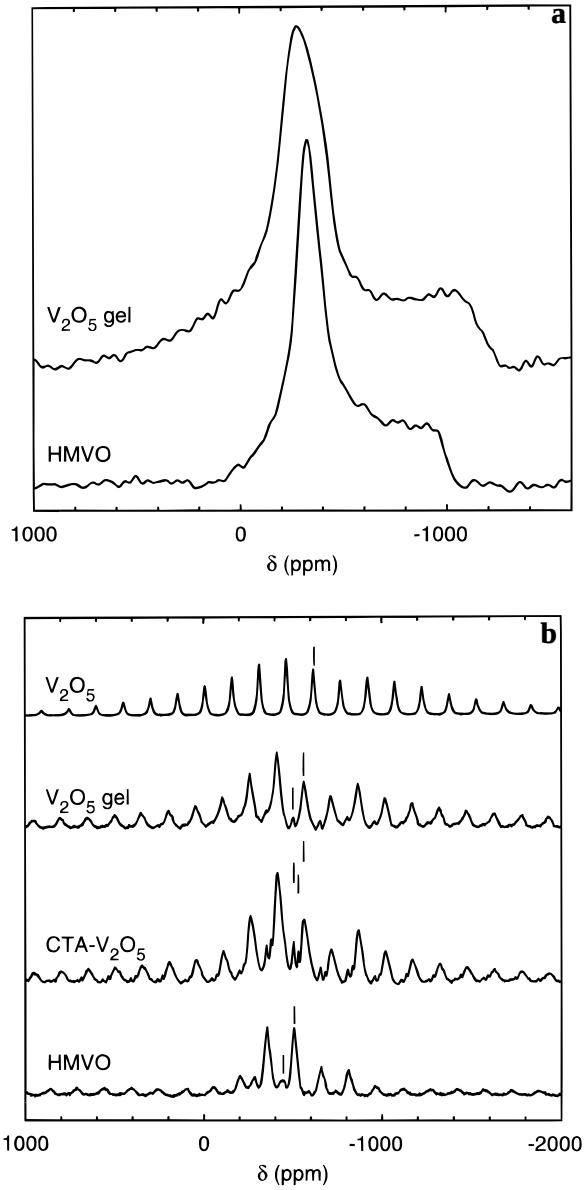

Figure 9. (a) ^{51}V solid-state static NMR spectra of V_2O_5 gel and hexagonal mesostructured vanadium oxide. (b) ^{51}V solid-state MAS NMR spectra of crystalline vanadium pentoxide, vanadium pentoxide xerogel, CTA−intercalated vanadium pentoxide gel, and hexagonal mesostructured vanadium oxide. Vertical bars represent the positions of the isotropic chemical shifts (uncorrected for second-order quadrupole perturbation) determined by recording spectra at a variety of spinning speeds. All other peaks are spinning sidebands.

Inasmuch as the MAS spectrum of a nucleus such as ^{51}V with $I = {}^7/_2$ and relatively small quadrupole moment is governed by both shift anisotropy and second-order quadrupolar effects, a particular chemical environment can only be precisely specified by accurate values of both the shielding tensor and quadrupolar coupling constant, the latter also being extremely sensitive to changes in structure. The extent of the quadrupolar coupling can be gauged qualitatively from the sideband pattern or analyzed in detail by simulation of the satellite lines.[32] The MAS NMR spectra of a series of vanadium oxide compounds are shown in Figure 9b. The spectrum of crystalline V_2O_5 exhibits an intense spinning sideband

(32) Skibsted, J.; Nielsen, N. C.; Bildsoe, H.; Jakobsen, H. J. *Chem. Phys. Lett.* **1992**, *188*, 405.

pattern arising from a significant quadrupole interaction and has a single isotropic shift at about −617 ppm in agreement with the values published in the literature. The anisotropy in the powder pattern (not shown) is about 970 ppm. The spectrum of the V_2O_5 gel contains a broad isotropic shift at −559 ppm, and the powder spectrum (Figure 9a) has an anisotropy of 882 ppm. There is also a sharp weak feature in the spectrum that is due to a minor amount of ammonium hexavandate impurity. We note that the chemical shift of the gel is unaffected by intercalation with CTA^+ as shown by the spectrum of CTA−V_2O_5.

The MAS NMR spectrum of HMVO has a major component with an isotropic shift at −505 ppm that is considerably more positive than that observed in either the gel or the crystalline vanadium oxide. Also there is a noticeable reduction in the intensity of the spinning sideband pattern compared to these other compounds. This indicates a reduction in the quadrupole interaction parameter for the vanadium nucleus in the HMVO compared to the V_2O_5 samples. Therefore although the vanadium coordination in HMVO appears to be square pyramidal as in V_2O_5, the distortion appears to be somewhat less.

FTIR/Raman. The FTIR spctrum of HMVO (Figure 10a) has only a superficial resemblance to that of the CTAV5 (CTAV−V10) salt (Figure 4a) although it is less well resolved and the envelope of vibrations around 980 cm^{-1} are displaced to slightly higher frequencies. Indeed, decomposition of the envelope of vibrational bands (inset) gives bands at 972, 988, 999, and 1031 cm^{-1}, and these are significantly displaced from those of CTAV5 or published vibrations of V10 salts.[31] The V═O vibration is Raman active, giving an intense band around 980 cm^{-1} that is often used to characterize vanadium oxide phases. As is evident from Figure 10b, the Raman spectrum of HMVO is almost identical with that of both gel and crystalline forms of V_2O_5, indicating that V═O units are indeed present in HMVO and that the V═O bond strength is comparable to that of bulk oxide phases. The Raman spectrum of HMVO with a single vibration in the 960−1100 cm^{-1} region is radically different from that of CTA−V10 which gives a series of bands, the most intense of which occur at 925 and 993 cm^{-1} (Figure 4b). Therefore, Raman and to a lesser extent FTIR spectroscopy argue for a vanadium coordination in the HMVO phase that is at least in part also similar to that of gel and crystalline forms of V_2O_5.

X-ray Absorption Spectroscopy. The near-edge structure at the vanadium k-edge contains information on vanadium coordination. The preedge structure arises from transitions of the photoelectron to bound states in this case 1s → 3d. When the vanadium coordination changes from five, such as in V_2O_5, to four, such as in $CrVO_4$ or NH_4VO_3, the preedge peak shifts down in energy by 0.6 to 0.8 eV.[33] There is also a progressive shift of this preedge peak to lower energy as the average oxidation state decreases.[34] The XANES spectra of CTA−vanadate, HMVO, and for comparison crystalline V_2O_5 are shown in Figure 11a. The difference in preedge peak energy is 0.22 eV between crystalline V_2O_5 and HMVO and 0.63 eV between V_2O_5 and CTAV. This shows that the V coordination in the CTA−vanadate is tetrahedral while in the HMVO compound the coordination number is closer to five than four. It is unlikely that the observed shift originates from an oxidation state change as EPR measurements have shown that none of these materials contain any significant amounts of V^{4+}.

In addition to the energy shift, the intensity of the 1s → 3d transition can also provide information on coordination number. The intensity of this transition is proportional to the square of the magnitude of the distortion away from centrosymmetry of the local structure about the absorber and is therefore greater for tetrahedral sites than it is for square pyramidal and octahedral sites. Titanium in different coordination appears to plot in distinctive regions of normalized preedge intensity versus absolute energy position plots.[35]

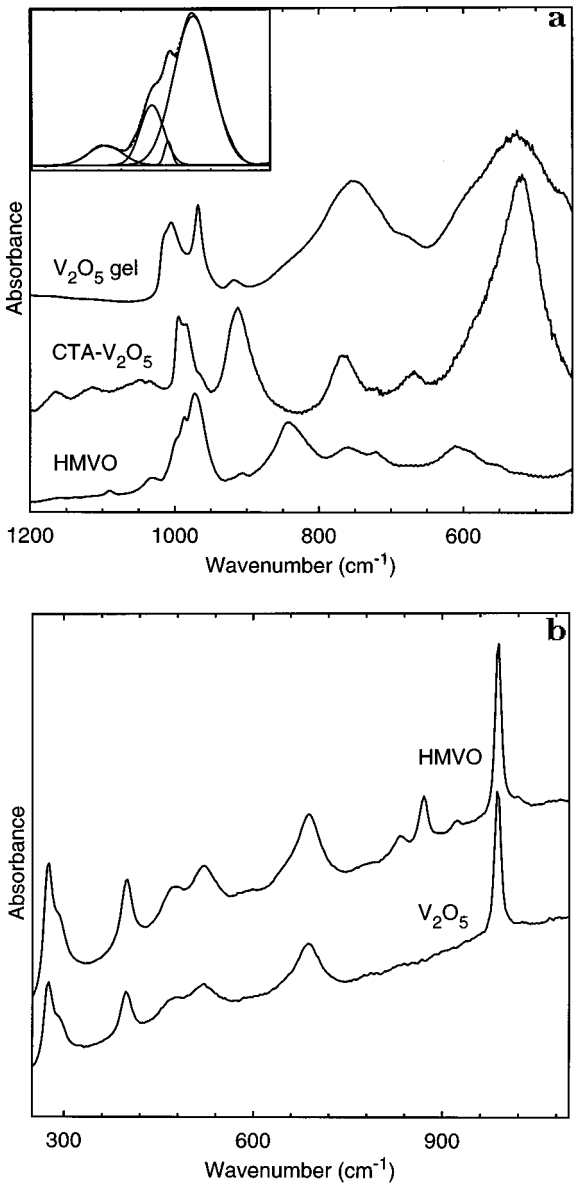

Figure 10. (a) FTIR spectra of vanadium pentoxide xerogel, hexagonal mesostructured vanadium oxide, and CTA−intercalated vanadium pentoxide xerogel. Inset: Spectral decomposition of the 920−1080 region of the spectrum hexagonal mesostructured vanadium oxide. (b) Raman spectra of hexagonal mesostructured vanadium oxide and crystalline vanadium pentoxide.

(33) Nabavi, M.; Taulelle, F.; Sanchez, C.; Verdaguer, M. *J. Phys. Chem. Solids* **1990**, *51*, 1375.

(34) Wong, J.; Lytle, F. W.; Messmer, R. P.; Maylotte, D. H. *Phys. Rev. B* **1984**, *30*, 5596.

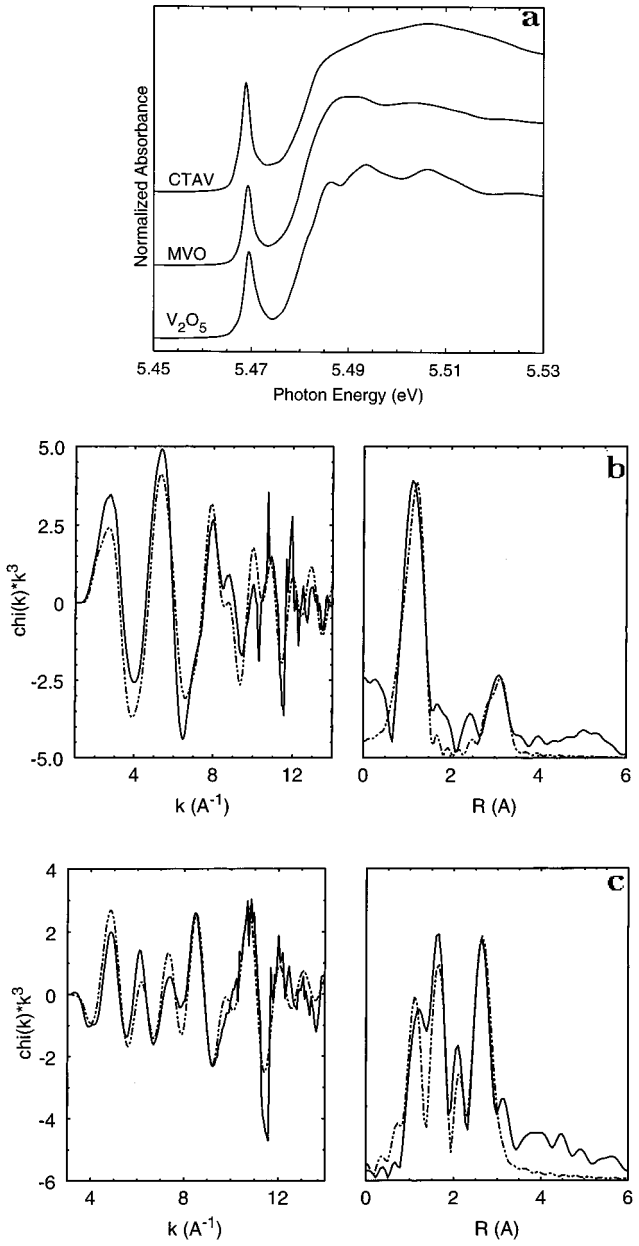

Figure 11. (a) XANES spectra of (a) CTA−vanadate, (b) hexagonal mesostructured vanadium oxide, and (c) crystalline vanadium pentoxide. (b) Experimental (solid line) and calculated (dotted line) k^3-weighted V k-edge EXAFS spectrum of CTA−vanadate (left) and magnitude Fourier transform of EXAFS data (right). (c) Experimental (solid line) and calculated (dotted line) k^3-weighted V k-edge EXAFS spectrum of hexagonal mesostructured vanadium oxide (left) and magnitude Fourier transform of EXAFS data (right).

This does not seem to be the case at the vanadium k-edge. So far normalized intensity values of 0.46,[37] 0.65,[36] 0.76,[34] and 0.74[33] have been reported for the preedge peak of crystalline orthorhombic V_2O_5. We have obtained a value for V_2O_5 of 0.60 which falls to the lower end in this range. Assuming that all these results have been obtained taking care to avoid thickness effects, we can only suspect that the variation in preedge intensity may be due to varying crystallinity of the various samples which gives variation in fwhm. Indeed this would seem to have some validity when the fwhm values are compared alongside the normalized intensities. It is also possible that experimental factors contribute to the observed variation. On the basis of the above argument we refrain from drawing any definite conclusion regarding coordination number based on normalized preedge peak intensity.

Table 2. EXAFS Simulation Parameters for Vanadium Compounds

compd	scatterer	*N*	*R* (Å)	$2\sigma^2$ (Å^2)
CTAV	O	2.9	1.70	0.005
	V	1.0	3.34	0.004
HMVO	O	1.5	1.68	0.001
	O	1.3	1.95	0.009
	V	1.3	3.08	0.004

The EXFAS and Fourier Transform (FT) EXAFS of the CTAV-vanadate and HMVO are shown in Figures 11b and 11c, respectively. For the CTA−vanadate sample (Figure 11b) the FT EXAFS is dominated by a single shell and the EXAFS could be simulated using the parameters listed in Table 2. The presence of a small but perceptible second-shell contribution is consistent with the connectivity in which one oxygen is shared (i.e. Q^1) which supports the conclusions from the NMR data. The V−O distance of 1.70 Å is close to that expected for vanadium in tetrahedral oxygen coordination. For the HMVO compound, a satisfactory simulation required the fitting of two oxygen and one vanadium shells. The first oxygen shell occurs at 1.68 Å, close to the V=O distance in crystalline V_2O_5. The second shell of oxygen atoms occurs at a distance of 1.95 Å which is slightly longer than the observed average in plane V−O bond distance in crystalline V_2O_5. The total number of oxygen atoms in the first two shells is quite low. At best the coordination number can be determined to about 20% by EXAFS but strong correlations between N and σ in the present analysis means that in reality much larger uncertainty can be attached to the coordination numbers. The presence of the vanadyl bond suggested by the EXAFS data of the HMVO compound is in agreement with the vanadyl vibration found in the Raman spectrum of both HMVO and crystalline and gel forms of V_2O_5 but the remainder of the bonding appears quite different. This may be due to the need for the extended vanadium oxide network to undergo quite severe curvature.

The data presented in this paper provide a more detailed characterization of HMVO, the synthesis and partial characterization of which we communicated recently.[19] Important issues in this regard are the coordination and degree of condensation of vanadium or, in other words, the structure of mesophase walls. Stein et al.,[13] in studying the cetyltrimethylammonium tungstate system, raised the possibility that materials giving TEM images reminiscent of M41S materials could be composed of uncondensed metatungstate polyanions arranged around cationic surfactant clusters. Their evidence for this was that IR spectra of their products closely resembled those of $H_2W_{12}O_{40}^{6-}$ Keggin anions. Moreover, the XRD patterns of their CTA−polytungstate salts were indexed on a monoclinic unit cell rather than the hexagonal or cubic unit cells usually found for M41S materials. We therefore first address the possibility that the HMVO materials have a similar

(35) Farges, F.; Brown, G. E.; Rehr, J. J. *Geochim. Cosmochim. Acta* **1996**, *60*, 3023−3038.
(36) Cartier, C.; Tranchant, A.; Verdaguer, M.; Messina, R.; Dexpert, H. *Electrochim. Acta* **1990**, *35*, 889−898.
(37) Prouzet, E.; Cartier dit Moulin, C.; Villain, F.; Tranchant, A. *J. Chem. Soc., Faraday Trans.* **1996**, *92*, 103.

structure and what bearing this might have on the poor thermal stability we observed on its calcination.[19]

At the outset it is clear that the HMVO has spectroscopic features which distinguish it from those of both the published data for decavanadate salts and the CTA−V10 salt synthesized here. We conclude further from NMR data that the mesostructured phase has a vanadium coordination and connectivity that is similar to that of vanadium pentoxide, which is quite different from that found for V10 species.

The presence of the V═O moiety in the final product is likely to be the cause of the poorly condensed nature of HMVO, and this presumably contributes to the poor thermal stability. Another factor contributing to the poor thermal stability could be the high surfactant/vanadium ratio of the products which results in a thin oxide wall. In M41S syntheses, different products are produced depending on the surfactant/silicate (Surf/Si) ratio.[41] Surf/Si molar ratios <1 give hexagonal phases, Sur/Si = 1−1.5 give cubic phases, and lamellar phases are favored by Surf/Si = 1.2−2. Irrespective of the final structure, the Surf/Si ratio of the product is always much lower than that of the initial solutions and is typically about 0.25. For the present samples, the Surf/V ratio of the product is much greater than that obtained for M41S materials and does not decrease greatly from the precursor to product. One alternative method for synthesizing more stable materials might be to use a precursor with lower Surf/V ratio, that is, salts having vanadate counterions with low charge and high nuclearity, which are not yet available synthetically. Another possibility for decreasing Surf/V could be through titration with the weak acid, $VOSO_4$, rather than a strong acid such as HCl. This raises the possibility of reactions between $VO(H_2O)^{2+}$ and $(EtO)_2VO_2^-$

$$VO(H_2O)_4^{2+} \rightarrow VO(H_2O)(OH)_2 + 2H^+$$

$$VO(H_2O)(OH_2)_2 + (HO)_2^{2-} \rightarrow [(OH)_2OV{-}O{-}VO_2(OH)]^{2-} + H_2O$$

which would result in a net decrease in Surf/V.

3. Mechanism of Formation of HMVO. The nature of the vanadium species present in solution during the synthesis of HMVO was investigated by recording ^{51}V solution NMR spectra of aliquots taken from the ethanolic CTAV solution at regular intervals during the titration. The initial solution prior to the addition of any acid contains essentially a single peak at −556.7 ppm, which changes only after the addition of acid, shifting to −555.5 ppm on reaching pH = 5.0.

The most likely candidates for the predominant species present in ethanol prior to acid addition are tetrahedral vanadates: the monoester $EtOVO_2(OH)^-$ and diesters $(EtO)_2VO_2^-$ of ethanol, as vanadates are prone to behave in alcohols.[23] Higher vanadate oligomers such as the dimer, $V_2O_7^{2-}$, trimer, $V_3O_{10}^{5-}$, or tetramer, $V_4O_{13}^{6-}$ seem improbable, because the chemical shift for these species is quite different and independent of pH. For isolated monomeric vanadate, $H_xVO_4^{3-x}$ the chemical shift is pH dependent and ranges from about −540 to −560 ppm.[25] The chemical shift for the tetrahedral monoester $(EtO)VO_2(OH)^-$ is also pH dependent, since this ester has ionizable protons with pK_a in the pH range under study here. Its signal varies from −535 ppm to a limiting value of −555 ppm as the pH changes from 10 to 7. In contrast, the diester, $(EtO)_2VO_2^-$, having no ionizable protons, gives a chemical shift of −552 ppm that does not vary within this pH range.[23] Although the predominant species in the water−ethanol−CTA−vanadate system has a line width consistent with either species, the pH dependence most closely matches that of the diester. The chemical shift is about 3 ppm more negative than that observed for the diester as the sodium salt in water,[23] which could be ascribed to the influence of the positively charged surfactant headgroup with which the diester anion is associated, and/or solvent effects. Further evidence for the predominance of $(EtO)_2VO_2^-$ in the ethanolic CTAV solution comes from electrospray mass spectrometry which gives a negative mass of 173 mass units as the base peak, corresponding to the formula $C_4H_{10}VO_4$.

As the titration proceeds, it is also possible to identify four lower frequency peaks with intensity that never exceeds about 5 to 10% of the initial observable vanadium. The resonance that appears at −570 ppm in Figure 12a initially has a line width of about 142 Hz. The chemical shift remains unchanged on acid addition while the line width increases to about 400 Hz on reaching $R \sim 0.14$. The chemical shift is consistent with assignment to the protonated dimer $[H_2V_2O_7]^{2-}$ (V2) which cannot be further protonated, and therefore its chemical shift should not be affected by lowering pH. The V2 species could be formed by initial partial hydrolysis of the diester followed by oxolation to yield $H_2V_2O_7^{2-}$. These species are eventually consumed as R increases beyond 0.6. The two broad resonances at about −575 and −585 ppm are probably due to the cyclic tetramer with a possible contribution from the trimer and pentamer not being excluded. Finally, the nature of the very broad resonance at about −600 ppm remains uncertain although $[VO_2]_n^{n+}$ species that have been identified in acidic solutions have chemical shifts close to this value.[26]

To determine whether all the vanadium present could be detected by solution NMR, we compared the signal intensity of aqueous vanadate solutions containing exclusively HVO_4^{2-} with ethanolic CTAV. From this we deduced that for the 35 mM ethanolic CTA−vanadate solution more than 80% of the total vanadium present is being observed. The absence of any significant broadening of the diester resonance in the initial solution at room temperature and above suggests that this particular solution is isotropic with respect to the vanadate diester. In contrast, the formation of a rod micellar liquid crystalline phase would be expected to cause, among other changes, major temperature-dependent line broadening in the spectrum, as has been reported for lyotropic liquid crystalline bilayer systems

(38) Tracey, A. S.; Radley, K. *Can. J. Chem.* **1985**, *63*, 2181.
(39) Henry, M.; Jolivet, J. P.; Livage, J. *Structure Bonding* **1992**, *77*, 155.
(40) Firouzi, A.; Kumar, D.; Bull, L. M.; Besier, T.; Sieger, P.; Huo, Q.; Walker, S. A.; Zasadzinski, J. A.; Glinka, C.; Nicol, J.; Margolese, D.; Stucky, G. D.; Chmelka, B. F. *Science* **1995**, *267*, 1138.
(41) Vartulli, J. C.; Schmitt, K. D.; Kresge, C. T.; Roth, W. J.; Leonowicz, M. E.; McCullen, S. B.; Hellring, S. D.; Beck, J. S.; Schlenker, J. L.; Olson, D. H.; Sheppard, E. W. *Chem. Mater.* **1994**, *6*, 2317.

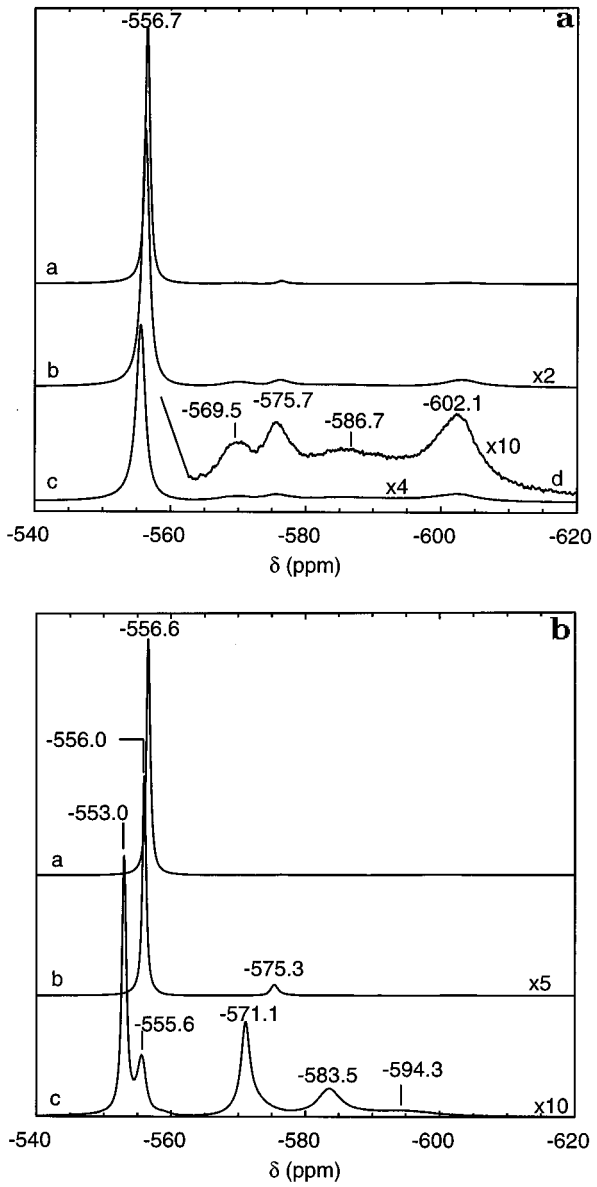

Figure 12. (a) Solution ^{51}V NMR spectra of suspensions obtained after adding 0.20 M HCl solution corresponding to (a) 0.010, (b) 0.045, and (c) 0.14 mole fractions of added water. Numbers above peaks are the chemical shifts with respect to $VOCl_3$. (b) Solution ^{51}V NMR spectra of suspensions obtained after addition of (a) 0, (b) 0.046, and (c) 0.444 mole fractions of distilled water. Numbers above peaks are the chemical shifts with respect to $VOCl_3$.

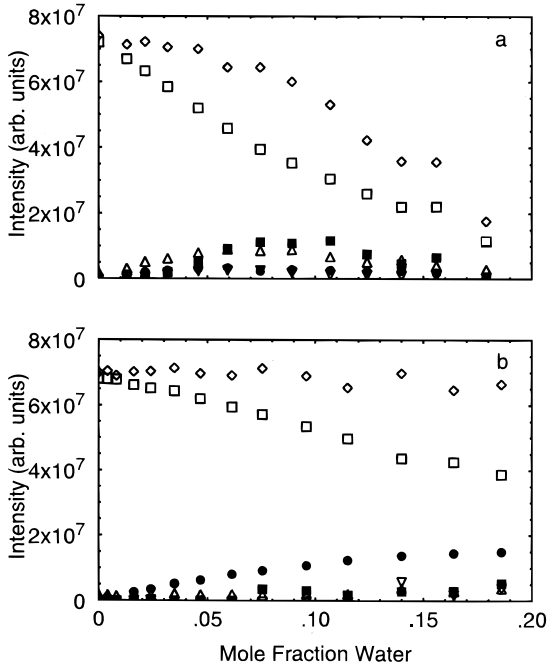

Figure 13. (a) Variation in the absolute intensity of ^{51}V NMR signals with mole fraction of water added as (a) 0.20 M HCl and (b) distilled water: ● = resonance at −576 ppm; ■ = resonance at −584 ppm; □ = resonance at −557 ppm; ▽ = resonance at −569 ppm; △ = −601 ppm; ◊ = total intensity.

where line widths of up to 2 kHz and resolved quadrupole splittings can be observed.[38]

The series of spectra resulting from the acid titration of ethanolic CTAV are shown in Figure 12a. It is apparent that there is a progressive disappearance of diester as acid is added although an additional minor resonance appears in the region between −560 and −650 ppm. This series of spectra were fitted with the minimum number of Lorentzian lines required to give a good fit and the peak positions and areas extracted. The data are plotted in Figure 13a as absolute spectral intensity for the various resonances as a function of added aqueous HCl and clearly show the disappearance of the diester and the evolution of a range of vanadate oligomers in addition to the putative $[VO_2]_n^{n+}$. The disappearance of the diester follows roughly the decrease in total observable vanadium. Although vanadate oligomers increase in intensity as titration progresses reaching a maximum at $R \approx 0.10$, they never contribute more than about 10% to the total intensity. During the titration, a solid phase is not observed visually until $R \sim 0.1$ (arrow in Figure 5). Although there is some decrease in the total observable vanadium up to this point, it decreases most markedly after precipitation first becomes evident. These observations suggest that the primary building blocks in the reaction to form HMVO do not appear to be the higher vanadate oligomers—V2 to V6—identified previously, because their concentration increases as the concentrations of diester and total observable vanadium decreases (Figure 13). The major point to emphasize here is that the loss of total NMR intensity with added acid occurs at the expense of the diester which must be converted rapidly and directly to species that are NMR invisible. Thus, a mechanism for the formation of HMVO must have as a key element the acid-catalyzed hydrolysis of the diester probably to form $VO_2(OH)_2^-$ species which are rapidly consumed to form large polymers. Furthermore, if the formation of HMVO necessitates the binding of anionic polyvanadates at the forming micelle interface, this would be expected to produce a slowing of reorientational motion sufficient to give a significant increase in line width. This is in fact what is observed in Figure 14 which shows a plot of the line width of the resonances from the diester (−556.7 ppm), V2 (−570 ppm), and V4 (−575 ppm) against the mole fraction of added water as aqueous acid. It can be seen that an R value of 0.06 is sufficient to cause at least a 3-fold increase in the line width of each of these three resonances. Since these line width increases occur prior to precipitation, it seems most likely that they are due to a slowing down of reorientational motions arising from cooperative micellization. During this process the diester and small V2

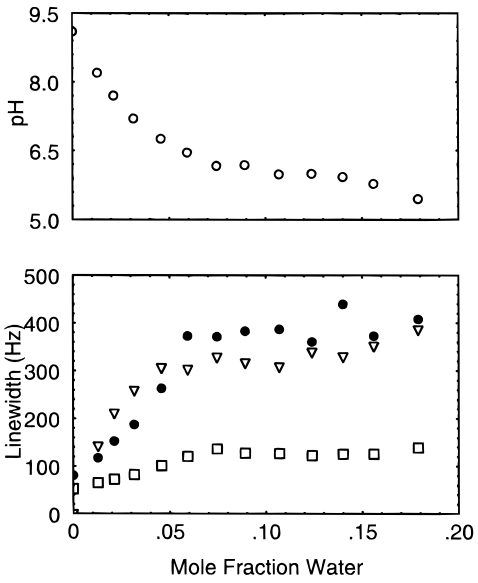

Figure 14. Top: Variation in solution pH with added acid. Bottom: Line width of ^{51}V NMR resonances of selected vanadate species: ● = resonance at −576 ppm; □ = resonance at −557 ppm; ▽ = resonance at −569 ppm.

and V4 vanadate counterions probably cluster at the surface of the forming micelles or small micellar aggregates. The higher vanadate oligomers whose NMR line width remains unaffected must eventually also condense directly with the growing mesophase as pH decreases or indirectly by providing an additional pool for the $VO(OH)_x$ species. This is mandated because the solution is eventually totally depleted of free vanadates. It is interesting to note that in the synthesis of vanadium pentoxide gels from acidified vanadate solutions neutral intermediates have been postulated which condense into linear chains.[39]

The mechanism being proposed here for the formation of HMVO is summarized in Figure 15 and involves the cooperative formation of both micelles and oligomeric vanadates and is in this sense similar to that postulated by Firouzi et al.[40] for the formation of mesoporous silicates.

To better understand the nature of the spectral changes occurring in the −560 to −650 ppm spectral region during acid titration, and the evolution of polyvanadates, we performed a parallel experiment titrating the ethanolic CTAV solution with water only, with the aim of distinguishing the effect of added water from that of aqueous acid. The spectra resulting from this experiment are shown in Figure 12b, while a plot of the peak areas is shown in Figure 13b. Unlike titration with HCl, the addition of water alone did not result in the precipitation of solid or loss of total signal intensity up to $R = 0.20$. Instead the solution became slightly turbid. A comparison of the line positions and intensities obtained from this data set shows that the changes occurring in the −560 to − 650 ppm spectral region are similar to the series obtained when HCl is the titrant with some important differences. When water is the titrant there is little change in the solution line widths and the species resonating at −570 ppm is absent. It seems highly likely therefore that it is the presence of water alone in the HMVO synthesis that causes the appearance of the vanadate oligomers. Another feature of this series of spectra is that the diester resonance gradually shifts from −556.6 ppm and splits into two resonances at −553.8 and −555.8 ppm after reaching an R value of 0.28 at which point the solution is only slightly turbid and no precipitate has formed. The CTA−vanadate solution becomes increasingly turbid when R reaches 0.50, and there is a 26% reduction in solution V concentration and a 28% loss in the amount of V observed by NMR. In other words, up to this point most of the vanadium is being observed. This indicates that, while the water is required to initiate hydrolysis of the diester, the acid is essential to catalyze the formation of HMVO.

To date a number of mechanisms have been put forward for the formation of mesostructured aluminosilicates that are still in dispute.[42] These include Beck et al.,[4] Vartuli et al.,[43] and Kresge et al.[45] who postulated two possible pathways for the formation of MCM-41. Pathway I involves first the formation of regular hexagonal micellar arrays followed by condensation of the silicate around the voids in this close packed structure. Pathway II (liquid crystal templating mechanism) involves first the formation of individual micellar rods which then become coated in silicate, finally condensing into a hexagonal array.[45] Of these two pathways, pathway I has been effectively eliminated because MCM-41 forms at surfactant concentrations well below cmc2 where hexagonal aggregates first form in surfactant/water solutions. Monnier et al.[46] subsequently postulated on the basis of TEM images that a lamellar intermediate is involved in the formation of MCM-41. Steel et al.[47] on the basis of ^{14}N NMR data have also proposed a mechanism involving a lamellar intermediate but have added the refinement that the intercalating species are rod micelles. Chenite et al.[48] have since shown that apparently lamellar phases observed by TEM are in fact hexagonal arrays viewed side on. Most recently Cheng et al.[49] have provided TEM data which they interpreted in a manner consistent with the liquid crystalline templating mechanism (pathway II). Monnier et al.[46] and Firouzi et al.[40] have refined the liquid crystalline templating mechanism to include the concept of cooperative formation of the mesophase upon addition of the inorganic phase and provided evidence for this mechanism. This was necessary because M41S phases can be, and usually are, formed in solutions in which the surfactant concentration is at or above cmc1 (spherical micelles) but well below cmc2 (sphere to rod transition). Thus to define the mechanism of formation one requires detailed snapshots of the state of molecular aggregation in the synthesis solution. Such information is not

(42) Raman, N. K.; Anderson, M. T.; Brinker, C. J. *Chem. Mater.* **1996**, *8*, 1682.
(43) Vartuli, J. C.; Schmitt, K. D.; Kresge, C. T.; Roth, W. J.; Leonowicz, M. E.; McCullen, S. B.; Hellring, S. D.; Beck, J. S.; Schlenker, J. L.; Olson, D. H.; Sheppard, E. W. *Studies Surf. Sci. Catal.* **1994**, *84*, 53.
(44) Kresge, C. T.; Leonowicz, M. E.; Roth, W. J.; Vartuli, J. C.; Beck, J. S. *Nature* **1992**, *359*, 710.
(45) Chen, C.-Y.; Burkett, S.L.; Li, H.-X.; Davis, M. E. *Microporous Mater.* **1993**, *2*, 27.
(46) Monnier, A.; Schuth, F.; Huo, Q.; Kumar, D.; Margolese, D. I.; Maxwell, R. S.; Stucky, G. D.; Krishnamurty, M.; Petroff, P. M.; Firouzi, A.; Janicke, M.; Chmelka, B. F. *Science* **1994**, *261*, 1299−1303.
(47) Steel, A.; Carr, S. W.; Anderson, M. W. *J. Chem. Soc., Chem. Commun.* **1994**, 1571.
(48) Chenite, A.; Page, Y. I.; Sayari, A. *Chem. Mater.* **1995**, *7*, 1015.
(49) Cheng, C.-F.; He, C.; Zhou, W.; Klinowski, J. *Chem. Phys. Lett.* **1995**, *244*, 117.

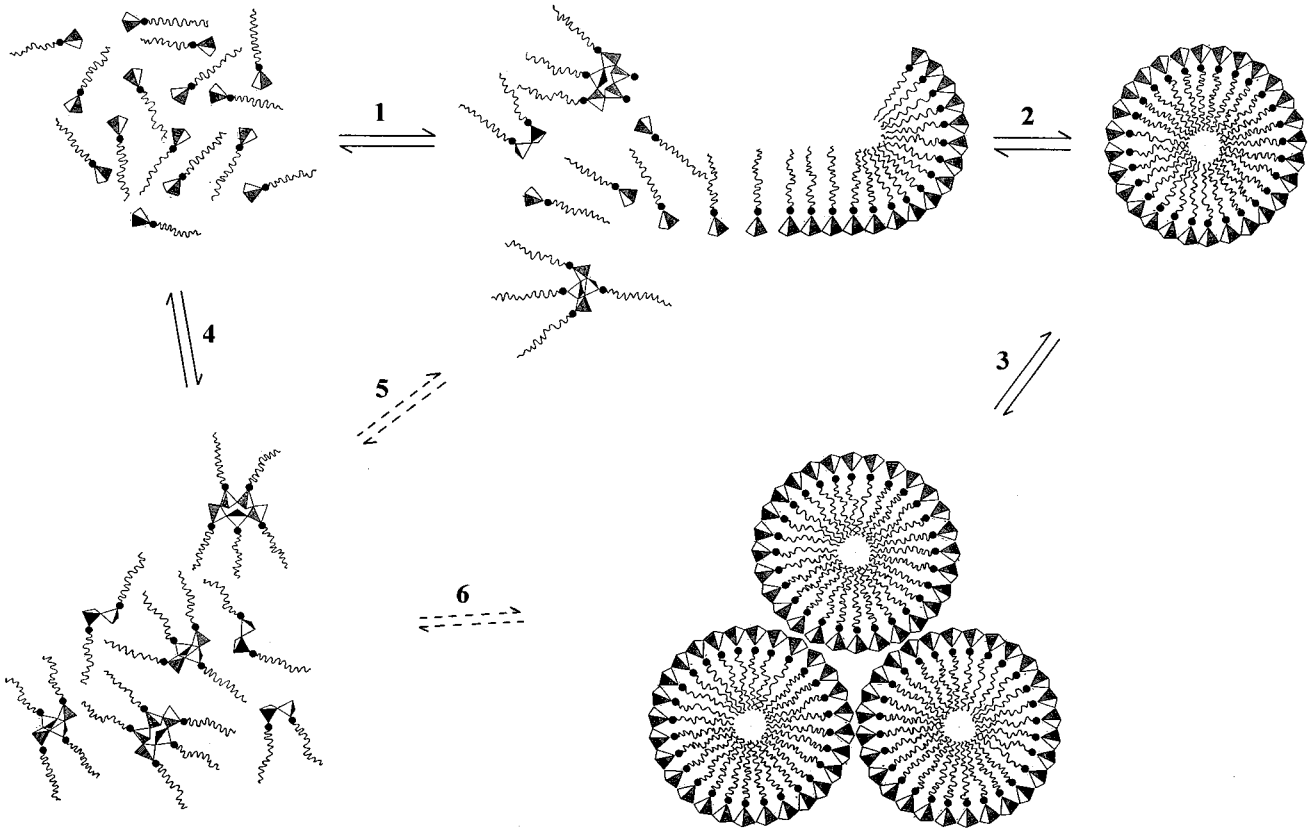

Figure 15. Schematic two-dimensional illustration of the essential features of the model for the formation of HMVO. Steps 1 and 2 involve the cooperative formation of rod micelles from an initial isotropic solution of mostly unaggregated surfactant molecules. Step 3 involves aggregation of micelles to form large aggregates. Step 4 depicts an additional reaction pathway producing larger vanadate oligomers that may contribute to micelle formation at step 1 and/or become accreted during the micelle aggregation at step 3. Note that the circular structures depicted in this two-dimensional illustration are sections of cylinders.

currently available but may be through the use of judicious isotopic labeling of the surfactant combined with NMR studies.

In the synthesis of HMVO a central issue is the state of molecular aggregation at time zero, i.e. prior to addition of acid. Phase diagrams of the closely related ternary water−ethanol−C_{16}TA−X system have been determined for X = Br^- and SO_4^{2-},[50] and at high molar ratios of ethanol, the solution is isotropic with only the L phase being observed. High molar ratios of surfactant are necessary to obtain the hexagonal E liquid crystalline phase. On the basis of the limited data available so far for ternary systems and assuming that the diester and oligomeric vanadate anions behave similarly to SO_4^{2-} the initial CTA−vanadate solution is expected to be isotropic and indeed the ^{51}V solution NMR data of this study corroborate this parallel. However, the NMR data also suggest that on addition of aqueous HCl there is a noticeable deceleration of reorientational motion of the diester and some of the smaller vanadate oligomers with relatively large slowly tumbling micellar structures that we presume are forming in solution. At this point the formation of a liquid crystalline phase comprising large aggregates of vanadate-encrusted micelles seems improbable as although the NMR line width increases substantially on acid addition, it is nonetheless relatively small and quadrupolar splittings such as those observed in genuine liquid crystalline systems[38] are not observed. These observations favor a mechanism involving the cooperative formation of micellar entities and oligomeric vanadate counterions from solutions which would normally not be expected to contain such species.[50] This micellization occurs in solutions with surfactant concentrations and containing solvents that would not normally be expected to give rise to large aggregate structures in a fashion similar to that proposed by Monnier et al.[46] and Firouzi et al.[40] for the formation of silicate M41S materials. Once the formation of an individual micelle is complete, however, spontaneous aggregation must be extremely rapid such that precipitation occurs with loss of NMR observable vanadium.

Vanadium pentoxide gels are normally synthesized spontaneously from aqueous decavanadic acid solutions,[26] and it has been proposed that the V10 ion provides the vanadium source, while the dioxovanadium cation VO_2^+ is consumed to form vanadate polymers which then condense to form the gel structure. In the present study there is no evidence for the formation of V10 which would be expected to predominate at high vanadium concentration and low pH (Figure 1a) and which are clearly not employed in our synthesis. Nor are VO_2^+ species observed, as they are in the case of vanadium pentoxide gel formation.[26] Our attempts to form a mesostructured phase by adding aqueous decavanadic acid solutions to solutions of surfactant always yielded a surfactant intercalated layered gel phase. It seems therefore that the presence of surfactant totally suppresses the formation of V10 species and are attributed to surfactant−vanadate interactions that are

(50) Fontell, K.; Khan, A.; Lindstrom, B.; Maciejewska, D.; Puang-Ngern, S. *Colloid Polym. Sci.* **1991**, *269*, 727.

strong enough to steer the reaction toward the formation of nonlayered mesophases.

Conclusions

HMVO can be formed in ethanolic solutions of CTAV by controlled addition of dilute aqueous HCl through processes which require the cooperation of water, acid and, surfactant. The resulting product has a structure similar to that of the hexagonal silicate mesophases, but the high surfactant-to-vanadium ratio suggests a narrow and therefore fragile wall structure which in turn may be responsible for the poor thermal stability of the material. In addition, the presence of V═O groups limits the degree of condensation of vanadate units within the walls of the mesostructure and this probably further contributes to the poor thermal stability. What is surprising therefore is not the poor thermal stability of HMVO but rather that this material can be made at all. Potential methods for producing more thermally stable mesoporous vanadium oxide materials have been discussed, but there is clear need for more extensive investigation.

The data presented in this study support the model we proposed earlier for the formation of the mesostructured vanadium oxide phase.[19] That is, that discrete vanadate species are initially present at the micelle interface as the only anionic species. Controlled addition of aqueous HCl initiates hydrolysis and condensation reactions in a regime where the anion concentration always favors vanadate and not the spectator anion, in this case chloride. This careful addition of aqueous HCl to the nonaqueous medium, together with the presence of the surfactant cation, perhaps serves to better control and direct what might otherwise be a cascade of runaway polymerization/condensation reactions. We surmise that increased connectivity of vanadium polyhedra occurs in conjunction with micellization and that the eventual condensation of vanadium-coated micelles leads to a wall structure in which the vanadium has a distorted octahedral coordination similar to vanadium pentoxide. Studies aimed at testing the above hypothesis are currently in progress.

Finally, ^{51}V solution NMR has considerable diagnostic capability due to the 100% natural abundance, good sensitivity, and relatively small quadrupole moment of the vanadium-51 nucleus. This technique has furnished detailed information on solution speciation from which a mechanism of formation has been proposed. Future studies should be directed toward gaining a more detailed molecular picture of the ternary system at low water concentrations before visible precipitation has occurred in order to confirm the existence of vanadium-containing mesophases. Such information can possibly be provided through isotopic labeling studies such as those reported by Firouzi et al.[40] for the case of silica−surfactant assemblies.

Acknowledgment. The authors are indebted to Professor Russell F. Howe of the School of Chemistry, University of New South Wales, under whose auspices this work was performed. We are grateful for the expertise of Dr. D. Jardine, Macquarie University, NSW, for the measurement of the electrospray mass spectra and Cristina Luca for art work. We are also grateful for the receipt of an Australian Research Council grant without which this work would not have been possible. Finally, acknowledgment is made to the Australian National Beam Line Facility and financial support from the Department of Industry, Science and Technology for EXAFS measurements.

CM960641M